Microsatellite Yaw-axis Attitude Control System Using Model Reference Adaptive Control Based PID Controller

Article *in* International Journal of Electrical and Computer Engineering Research · June 2024

DOI: 10.53375/ijecer.2024.389

CITATION
1

READS
32

2 authors:

Paulinus Chinaenye Eze
Imo State University
32 PUBLICATIONS **106** CITATIONS
SEE PROFILE

Isaac A. Ezenugu
Imo State University
67 PUBLICATIONS **97** CITATIONS
SEE PROFILE

Microsatellite Yaw-axis Attitude Control System Using Model Reference Adaptive Control Based PID Controller

Paulinus C. Eze*, Isaac A. Ezenugu
[1]Department of Electrical and Electronic Engineering, Imo State University, Owerri, Nigeria
Emails: eze.paulinus@imsuonline.edu.ng (Paulinus C. Eze), *ezenugu@imsu.edu.ng* (Isaac A. Ezenugu)
* *Corresponding author*

Abstract: **This paper presents a Model Reference Adaptive Control (MRAC) based Proportional Integral and Derivative (PID) controller for microsatellite yaw-axis Attitude Control System (ACS). The objective is to combine the algorithm of MRAC with PID to improve the performance of a microsatellite system especially settling time. MRAC based PID controller for yaw-axis ACS was modelled and simulated in MATLAB/Simulink to meet transient response characteristics specifications. The performance of the system was evaluated in terms of rise time, settling time, maximum overshoot, and steady-state error including energy consumption measured based on armature voltage of the direct current motor. The simulation results revealed that the proposed system meets all the performance specifications and outperformed classical PID controller for adaption gain of 0.2 to 20. When compared with PID and Proportional Derivative (PD) based Controllers in previous study for adaption gain of 10, 15, and 20, the proposed system proved to be superior. Generally, the choice of the MRAC based PID controller considering the range of adaption gain (γ = 0.1 to 20) should be based on either transient response advantage or energy consumption or even both over PID controller. The significance of this study is that an MRAC based PID controller that offered wide range of adaption capability for microsatellite ACS has been proposed.**

Keywords: **Attitude control system, Microsatellite yaw-axis, Model reference adaptive control (MRAC), PID controller**

I. INTRODUCTION

There is critical demand for high-precision Satellite Attitude Control (SAC) and the need for satellite control technique that will ensure system reliability, stability and accuracy is becoming increasingly stringent considering the rapid development in aerospace industry [1,2]. A satellite in its on-orbit flight will experience pitch, yaw, and roll variations because of external disturbances and gravitational influence. The effect of the action of these disturbances on the satellite can result in its displacement over time and as such resulting to the angular variation in pitch, yaw and roll [3]. Thus, it is important to have a subsystem that provides the needed manoeuvring to ensure that an on-orbit flight satellite is maintained at a predetermined position and a defined attitude in order to achieve expected task and meet designed specifications or performance standards. On account of this, satellite attitude control system (SACS) is integrated with a controller that serves as the subunit providing the needed manoeuvring capacity to keep the satellite in its defined orientation for effective flight operation. However, to effectively accomplish its tasks, it is critical to study the satellite's control subsystem in order to choose the appropriate control algorithm that offers improved dynamic or transient behaviour and steady-state performance for flight attitude adjustment and stability.

Several control schemes have been developed for stabilizing attitude motion. Linear control techniques that largely depend on feedback from output such as the classical Proportional Integral and Derivative (PID) controllers have been well implemented as subsystem for Satellite Attitude Control SAC. For instance, classical PID controller was used to meet performance specifications in yaw angle control of satellite system [4], while Integral Time Absolute Error (ITAE) based PID controller and Proportional and Derivative (PD) controller have been used for stabilizing attitude motion for microsatellite yaw-axis [5]. The performance of Linear Quadratic Regulator (LQR) and PID control algorithm when employed in the on-orbit stabilization of a Low Earth Orbit (LEO) satellite attitude by [6] revealed that the PID controller was unable to stabilize the system after 500 s, whereas the LQR achieved the design criteria for the roll, pitch and yaw-axis attitude. In the study regarding SAC, PID control algorithm and fuzzy-PID based controller were applied with the results revealing that the system achieved steady state faster with PID than fuzzy-PID but some torque oscillation whereas the Fuzzy-PID provided smother and better stable transient and steady state response performance [1]. Attitude control of satellites was achieved using variable structure PID controller, which integrates the classical PID algorithm, trajectory panning, variable structure and fault tolerant [2]. The performances of Fuzzy Logic Controller (FLC), conventional PID controller, and modified PID controller were experimentally compared in a laboratory nanosatellite and its testing system with the results showing that using FLC rather than PID yielded significant improvement in energy consumption, convergence time and robustness in accordance to changes in environmental condition, which were the performance criteria including steady state error (accuracy) [7]. Also, the performance of a satellite in a circular orbit with four CMGs in pyramidal configuration has been evaluated either by employing Exponential Mapping Control (EMC) or Linear

Quadratic Tracker (LQT) with integral compensator [8]. Selectable gains PID controllers were used for a generic model of a nanosatellite attitude control and stabilization system whose performance was evaluated in three modes of operations namely, detumbling after isolation from the launcher, nominal operation when the satellite attitude is subjected to slight or moderate perturbation, and momentum unloading following reaction wheel saturation [9]. Direct Torque Control (DTC) based scheme that uses PID algorithm to compute the demand torque to actuator from the error between the desired attitude and estimated attitude and followed by DTC on the actuator for stabilizing pitch, roll and yaw angles of satellite ACS was implemented in [10]. Control system for tracking of satellite attitude was achieved using control algorithm based on Lyapunov stability control theory in [11]. Three-axis stabilization control and pointing stabilization control of under-actuated spacecraft attitude with two reaction wheels was achieved using an integrated control technique based on dual-mode Model Predictive Control (MPC) and utilizing solar radiation pressure from two solar panels [12]. Classical PID controllers have been largely employed in many studies relating to satellite attitude control system and generally in several industrial process control operations because of its associated simple structure and design simplicity including the ability to provide control effort for system with complex dynamics. Despite the advantages of classical PID controllers, their performances are largely affected by mismatch or parameter variation [13]. In nanosatellite ACS, PID controllers shown weakness of relatively long area of little variation phase prior to correcting the final sate in some manoeuvres and was unable to stabilize LEO satellite attitude after 500 s which is beyond allowable practical value [6,7]. Intelligent based control such as FLC and fuzzy-PID have been proposed to replace PID controllers. This can be attributed to the fact that heuristic information are used by FLC to offer realistic and expedient alternative to addressing nonlinear problems related to control systems [14]. However, the use of FLC controller only results in steady-state error [13,15] while expert PID and fuzzy-PID controllers on the other hands, always have sub-par timing precision and limited anti-interference capabilities [16]. Even though CMGs are satellite attitude control actuators that act as torque amplifier and suitable for three-axis slew manoeuvring, the drawback of the scheme is the possibility of singularities for certain gimbal angles combination [17]. LQR and LQG controllers have the ability to provide optimal control to system performance with improved settling time and almost zero overshoot (or oscillation), but the optimal gain matrix has fixed parameters just like the conventional PID controller, and subject to system mismatch.

Contrary to PID controller, whose control is only governed by the value of actual output of the system based on feedback mechanism, MRAC is governed by the difference between the system's actual output and the out of the reference model. Thus, the goal is to meet the design specifications of a microsatellite yaw-axis ACS while reducing position deviation or error to zero with improved system stability and ensuring that the orientation accuracy is maintained using MRAC based PID controller with approximated second order model that is capable of providing a suitable unique adaption potential via a wide range of adaptation gain to on-orbit flight satellite with respect to yaw angle stabilization.

II. System Design

In this paper, the MATLAB codes and the Simulink embedded blocks were the main tools used for the modelling of microsatellite yaw-axis ACS, design of MRAC based PID controller and simulation. The open and the closed loop transfer functions, and the referenced model were determined using the MATLAB codes. The parameters of the transfer functions of the various components of the system (PID controller, MRAC, amplifier, actuator, and satellite structure) were entered into the embedded blocks of the developed Simulink model used for simulations.

A. Modelling of Yaw-axis Attitude Control System

This subsection deals with the description of a microsatellite and is presented in terms of closed loop network of ACS including the performance criteria of the system, which are established in terms of overshoot, settling time, and steady state error. Also, the design of the system in terms of the method used to achieve the performance objectives such as maximum overshoot ($M_p \leq 5\%$), settling time ($t_s \leq 2\,s$) with 2% criterion, zero steady-state error for a microsatellite yaw angle control system [5].

The closed loop description of a microsatellite yaw-axis ACS studied in [5] is shown in Fig. 1. It is a Single Input Single Output (SISO) linear time-invariant (LTI) system with unity feedback gain. With the block diagram arrangement, the microsatellite yaw-axis ACS can be vividly described in a very simplified manner. Thus, as shown in Fig. 1, during the on-orbit flight of the satellite, an attitude manoeuvre takes place which involves the controller sending a control signal to the amplifier in order to boost the signal strength (via increase in magnitude) and the amplified signal (which is the motor armature voltage) reaches the actuator (motor) that produces a proportional output that is sufficient enough to adjust the satellite structure (plant) orientation in terms of yaw angle in this case, according to the error signal (which is the difference between the desired (target) attitude and the actual attitude measured by the feedback sensor). Generally, the attitude controller is designed to align the actual attitude (yaw angle) to a desired attitude (or target angle). The desired attitude can be pointing in fixed direction (that is static orientation) or dynamic with respect to time [7].

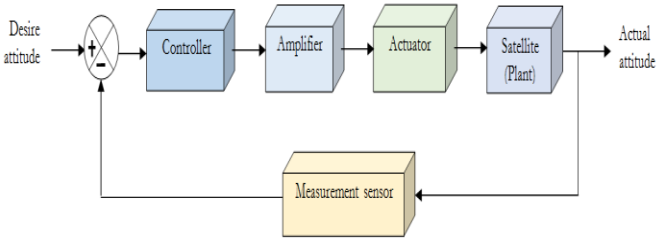

Fig. 1. Block diagram of attitude control loop

The dynamics of the amplifier, actuator and the satellite

structure are determined in terms of transfer functions in Laplace transform (s-domain) given by [5]:

$$G_{sat}(s) = \frac{1}{0.8\,s^2} \tag{1}$$

$$G_a(s) = \frac{78.3\,s}{s^2 + 1815.4\,s + 24466} \tag{2}$$

$$G_{amp}(s) = \frac{240}{0.1\,s + 1} \tag{3}$$

where $G_{sat}(s)$ is the satellite structure (plant) dynamic, $G_a(s)$ is the actuator dynamic, and $G_{amp}(s)$ is the amplifier dynamic. The MATLAB/Simulink model of the system (without controller) regarding (1) to (3) is shown in Fig. 2.

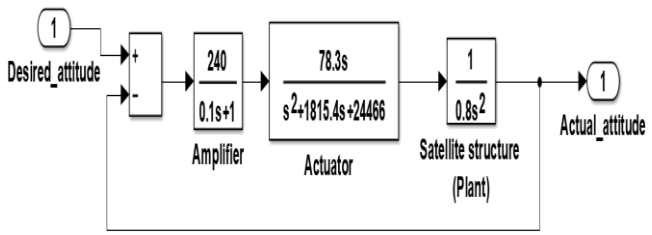

Fig. 2. System model without controller in MATLAB/ Simulink

The cascade combination of (1) to (3) gives the forward path gain expressed in (4) for the closed loop control system in Fig. 1 neglecting the controller. Substituting the numerical values of the transfer functions and using software (i.e., MATLAB) to solve (4), gives (5).

$$G(s) = G_{amp}(s) \times G_a(s) \times G_{sat}(s) \tag{4}$$

$$G(s) = \frac{18792\,s}{0.08\,s^5 + 146\,s^4 + 3410\,s^3 + 1.957\times10^4\,s^2} \tag{5}$$

Equation (5) shows that the overall dynamic for yaw-axis attitude determination for the microsatellite is 5th order system considering the individual component (amplifier, actuator and satellite structure) transfer function. Thus using the classical definition for transfer function of a negative feedback closed loop control system (without the controller) in (6), the numerical value for uncontrolled closed loop transfer function of the system is computed using MATLAB and it is given by (7).

$$\frac{\theta_y(s)}{\theta_d(s)} = \frac{G_{amp}(s) \times G_a(s) \times G_{sat}(s)}{1 + [G_{amp}(s) \times G_a(s) \times G_{sat}(s)] \times H(s)} \tag{6}$$

$$\frac{\theta_y(s)}{\theta_d(s)} = \frac{18792\ s}{0.08\,s^5 + 146\,s^4 + 3410\,s^3 + 1.957\times10^4\,s^2 + 18792\,s} \tag{7}$$

where, $\theta_d(s)$ is the desired attitude (target yaw angle), $\theta_y(s)$ is the actual attitude (current yaw angle), and $H(s)$ is the unity feedback gain of the measurement sensor.

B. Adaptive Control Based PID Model

This subsection establishes the control technique used in achieving yaw angle control for microsatellite system. The proposed system is a MRAC based PID algorithm with approximated second order reference model. There are several approaches to designing MRAC such as Lyapunov theory, augmented error theory, and Massachusetts Institute of Technology (MIT) rule. The MIT rule is used in this paper in modified form as in [18,19]. Designing the MRAC using modified MIT rule requires establishing the error and cost function for the adjustment mechanism and a reference model. Subsequently, a PID algorithm is established and integrated as the inner loop control scheme for the system. Figure 3 is the block diagram of the proposed system.

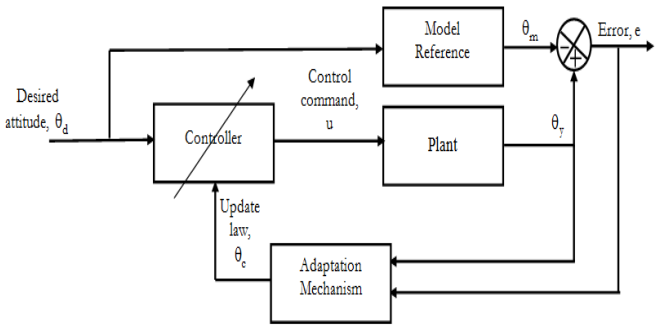

Fig. 3. Block diagram of proposed microsatellite yaw-axis attitude control system

Adaptation mechanism: Looking at Fig. 3, let the difference between the satellite actual yaw-axis attitude (i.e. yaw angle) θ_y and the output of the reference model θ_m be defined as error e given by:

$$e = \theta_y - \theta_m \tag{8}$$

The cost function J is represented in terms of Equation (8) by:

$$J(\theta_c) = \frac{1}{2}(\theta_y - \theta_m)^2 = \frac{1}{2}e^2 \tag{9}$$

where θ_c is the adjustable parameter. The cost function can be minimized in such a way that it tends to zero by adjusting θ_c in the direction that a negative gradient J is maintained [18,19] and this is defined mathematically by:

$$\frac{d\theta_c}{dt} = -\gamma \frac{\partial J}{\partial \theta_c} = -\gamma\, e \frac{\partial e}{\partial \theta_c} \tag{10}$$

Equation (10) is the expression for the change in θ_c with time in order to minimize the cost function $J(\theta_c)$ to zero. Also, $\partial e/\partial\theta_c$ is called the sensitivity derivative. The quantity γ (gamma) is a positive value that represents the adaption gain of the adjustment mechanism for the controller [18,19].

Suppose the microsatellite yaw-axis ACS is a linear process with transfer function $\beta G(s)$ where β is a parameter of unknown value. The objective is to design a reference model with known performance characteristics that the system will automatically follow or track irrespective of variations in system parameters or environmental perturbation. Now, let the reference model be approximated to a second order transfer function considering the fact that the satellite structure (plant) in (1) is a second order system. Therefore, the reference model $G_m(s)$ is defined by:

$$G_m(s) = \beta_o G(s) \tag{11}$$

where β_o is a parameter whose value is known. Hence, the error defined by Equation (8) can be re-defined as a transfer function in s-domain by:

$$E(s) = \beta G(s)\, U(s) - \beta_o G(s)\, U_c(s) \qquad (12)$$

where $\beta G(s)\, U(s) = \theta_y(s)$, $\beta_o G(s)\, U_c(s) = \theta_m(s)$, $U(s)$ and $U_c(s)$ are the control inputs to the system and the reference model respectively. Therefore, the control law is defined by:

$$U(s) = \theta_c \times U_c(s) \qquad (13)$$

The substitution of Equation (13) into Equation (12) and taking the partial derivative gives:

$$\frac{\partial E(s)}{\partial \theta_c} = \beta G(s)\, U_c(s) = \frac{\beta}{\beta_o}\theta_m \qquad (14)$$

Substitute Equation (14) into Equation (10), gives:

$$\frac{d\theta_c}{dt} = -\gamma e \frac{\beta}{\beta_o}\theta_m = -\gamma^1 e \theta_m \qquad (15)$$

where, $\gamma^1 = \gamma\beta/\beta_o$ and (15) is the update law for and represents the adjustment mechanism of the adaptive controller. The adaption gain was found to be in the range of $0.1 \le \gamma \le 20$.

Reference model: The reference model $G_m(s)$ is designed as a second order system, which is an approximated model to the overall transfer function of microsatellite yaw-axis ACS in (5), considering the fact that the plant $G_{sat}(s)$ is a second order system. It is expected that the proposed system meets the design specifications stated earlier for transient (dynamic) and steady-state performance. The second order reference model is defined by:

$$G_m(s) = \frac{{\omega_n}^2}{s^2 + 2\zeta\omega_n s + {\omega_n}^2} \qquad (16)$$

where, ω_n, ζ are the natural frequency and damping ratio. These quantities are determined by (17) and (18) as follow.

$$M_p = e^{-\pi\zeta/\sqrt{1-\zeta^2}} \qquad (17)$$

where, the maximum overshoot in percentage M_p is assumed to be 5%. Substituting this value into solving (17) gives: $(1-\zeta^2)^{1/2}\log_e(0.05) = -\pi\zeta\log_e^e \Rightarrow \zeta = 0.69$. The settling time t_s is assumed to be 1s. Thus, the natural frequency is computed using:

$$T_s = \frac{4}{\zeta\omega_n}, \qquad (18)$$

which, yields $\omega_n = 5.77 \text{rads}^{-1}$. Substituting these values into Eq. (16) gives the reference model as:

$$G_m(s) = \frac{33.3}{s^2 + 7.96s + 33.3} \qquad (19)$$

PID controller: The block diagram of a PID control system is shown in Fig. 4. The figure shows that the output of the PID controller $u_{pid}(t)$ is determined from the combined operations of the proportional integral and derivative elements, which are coordinated at the same time to carry out a correctional action called control command $u_{pid}(t)$ that changes the system into a new output state [14].

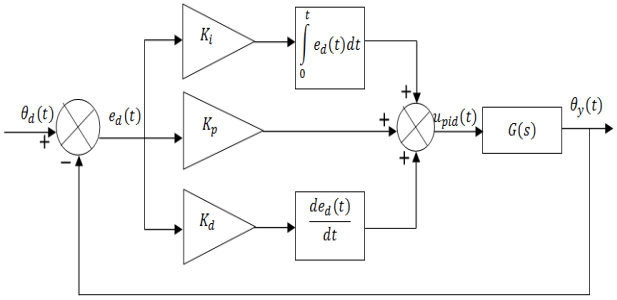

Fig. 4.Block diagram of PID control algorithm

The PID control algorithm can be determined by analysing Figure 4. The variables $\theta_d(t)$, $e_d(t)$, and $u_{pid}(t)$ are the reference input (i.e. the desired attitude), error (difference between desired attitude and the actual attitude $\theta_y(t)$), and the control variable. Also, K_p, K_i, and K_d are the PID parameters whose values determines action of the controller. Hence, as the error $(e_d(t) = \theta_d(t) - \theta_y(t))$ is fed into the PID, complex mathematical computation is executed by controller and the resulting output is given by:

$$u_{pid}(t) = K_p e_d(t) + K_i \int_0^t e_d(t)dt + K_d \frac{de_d(t)}{dt} \qquad (20)$$

Equation (20) is the classical PID command algorithm in time domain and can be defined in complex frequency domain (i.e. s-domain) assuming zero initial condition as:

$$u_{pid}(s) = K_p E_d(s) + K_i \frac{1}{s} E_d(s) + K_d s\, E_d(s) \qquad (21)$$

Equation (21) can be further simplified to give:

$$G_c(s) = K_p + K_i \frac{1}{s} + K_d s \qquad (22)$$

where, $G_c(s) = u_{pid}(s)/E_d(s)$ and is the PID control algorithm. The parameters of the designed PID controller are $K_p = 20.55$, $K_i = 0.0564$, $K_d = 1.98$. MATLAB/Simulink models of the PID control system and MRAC based PID controller are shown in Fig. 5 and Fig. 6.

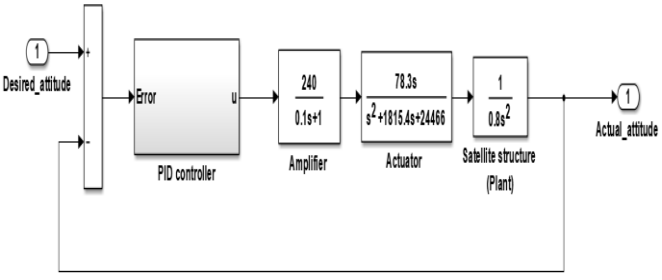

Fig. 5. System model with PID controller in MATLAB/ Simulink

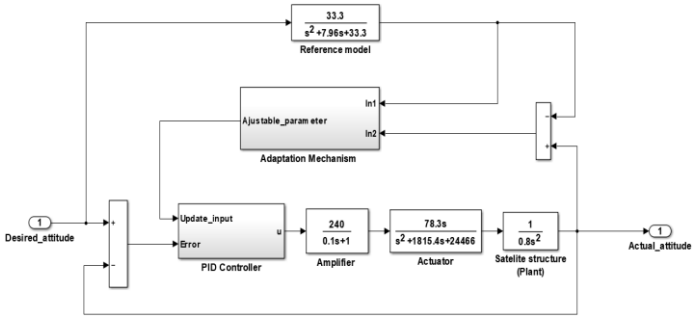

Fig. 6.System model with MRAC-PID controller in MATLAB/ Simulink

Optimal performance index: Performance index such as Integral Square Error (ISE), Integral Absolute Error (IAE), and Integral Time Absolute Error (ITAE) can be used to define the objective of the control system to mean the ability of it to guarantee that the satellite yaw-axis attitude move within the defined orientation with minimum error. Since the adaptive gain is of a very wide range, these optimal performance parameters have been used to evaluate the value(s) in order to determine the range of the adaption gain that provides the optimal performance in terms of minimized error. This is achieved in minimum time using a bounded control effort, which is defined within initial time t_0 to final time t_f and implemented using Simulink models. The mathematical expressions for ISE, IAE, and ITAE are given by:

$$ISE = \int_{t_0}^{t_f} e^2(t)dt \tag{23}$$

$$IAE = \int_{t_0}^{t_f} |e(t)|\,dt \tag{24}$$

$$ITAE = \int_{t_0}^{t_f} t\,|e(t)|\,dt \tag{25}$$

III. RESULTS AND DISCUSSION

The results of the analysis carried out regarding the performance of the system simulated in MATLAB/Simulink environment are presented in this section. Three subsections are used to clearly discuss the simulation results. Generally, the effectiveness of the system to maintain desired satellite yaw-axis attitude is considered to be the ability to track step angle of 1 degree while ensuring that the performance specifications are achieved as soon as possible including energy consumption efficiency and accuracy (measured in terms of steady state error).

A. System without controller

In the uncompensated (or absence of controller) scenario, the microsatellite was examined assuming there was no control algorithm introduced as a subsystem in the ACS to ensure that satellite yaw angle is stabilized and maintained at desired attitude with optimal tracking capacity while converging rapidly (i.e. attaining steady-state as quick as possible measured in terms of settling time) with very much little or zero oscillation (measured in terms of maximum overshoot). Figure 7 shows the uncontrolled system response.

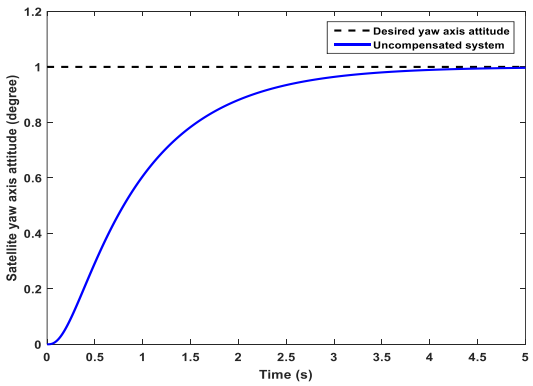

Fig. 7. Step response of uncontrolled system

The numerical analysis of the step response in Fig. 7 reveals that the system in the absence of controller has a transient and steady-state characteristics defined as follow: rise time (t_r) of 1.860 s, settling time (t_s) of 3.3658 s, peak time (t_p) of 5.0 s, maximum overshoot (M_p) of 0%, final value of 1 degree, and steady state error (e_{ss}) of 0 . The step response curve shows that in the uncompensated state (i.e. without controller), the system seems sluggish considering the rising time and was unable to be driven to the desired attitude at the predefined-time convergence (i.e. desired settling time). Therefore, there is need to implement a controller as a subsystem to improve system on-orbit flight performance with respect to the yaw angle.

B. MRAC based PID Control System

In this subsection, simulation results are presented for step response in terms of satellite yaw-axis attitude in degree for PID controller developed in this paper tagged PID (new) and the MRAC-PID controller with adaptive gain (gamma) of range $0.1 \le \gamma \le 20$ as shown in Figure 8(a) and (b). The numerical values in terms of transient and steady-state parameters are presented in Table 1. Other results from the simulation analysis are presented in terms of adjustable parameter values with respect to the adaptive gains shown in Figure 9(a) and (b) with numerical values shown in Table 2, error voltage shown in Figure 10(a) and (b), motor armature (actuator) voltage shown in Figure 11(a) and (b) and motor (actuator) torque shown in Figure 12(a) and (b). The numerical results shown in Figure 11 and 12 are presented in Table 3. Lastly, simulation was conducted in terms of ISE, IAE, and ITAE to certain the value(s) of gain at which the designed MRAC will provide the optimal results and are presented in Table 4. It should be noted that the MRAC-PID is tagged MRAC (Gamma) in the legends of the various simulation plots with respect to the adaption gains of the controller for simplicity.

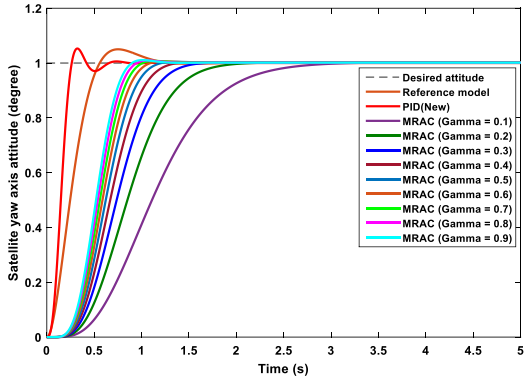

Fig. 8(a) Step response of PID and MRAC ($0.1 \leq \gamma \leq 0.9$)

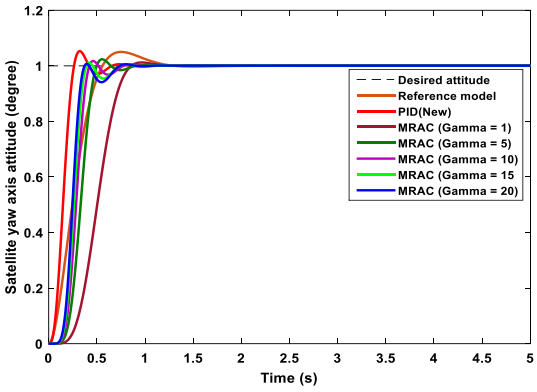

Fig. 8(b) Step response of PID and MRAC ($1 \leq \gamma \leq 20$)

TABLE 1.STEP RESPONSE CHARACTERISTICS OF PID AND MRAC-PID

System condition	t_r (s)	t_s (s)	M_p (%)	t_p (s)	e_{ss} (degree)
PID (New)	0.16	0.57	5.25	0.32	0
MRAC (gamma = 0.1)	1.32	2.53	0	5.00	0
MRAC (gamma = 0.2)	0.89	1.74	0	3.64	0
MRAC (gamma = 0.3)	0.72	1.40	0.02	2.04	0
MRAC (gamma = 0.4)	0.62	1.21	0.12	1.58	0
MRAC (gamma = 0.5)	0.56	1.09	0.28	1.36	0
MRAC (gamma = 0.6)	0.51	1.00	0.45	1.23	0
MRAC (gamma = 0.7)	0.47	0.94	0.63	1.14	0
MRAC (gamma = 0.8)	0.44	0.89	0.79	1.07	0
MRAC (gamma = 0.9)	0.42	0.84	0.94	1.01	0
MRAC (gamma = 1)	0.40	0.81	1.00	0.97	0
MRAC (gamma = 5)	0.22	0.58	2.27	0.55	0
MRAC (gamma = 10)	0.18	0.69	1.67	0.46	0
MRAC (gamma = 15)	0.16	0.67	1.07	0.42	0
MRAC (gamma = 20)	0.15	0.67	0.64	0.39	0

Looking at Table 1, it can be deduced that the control system based on PID (New) controller outperformed the MRAC based PID controller irrespective of the adaption gain (γ) in terms of reduced settling time and peak time. It also outperformed the MRAC based PID controller with γ = 0.1 to 10 in terms of rise time. For adaptation gain 15, the PID (New) controller and the MRAC based PID controller yielded equal rise time. However, for γ = 20, the MRAC based PID control system outperformed the PID (New) controller in terms of rise time. On the other hand, considering the maximum overshoot for the various system conditions, the MRAC based PID controller with γ = 0.1 or 0.2 yielded the best performance. Generally, the PID (New) controller did not meet all the required system specifications (having overshoot > 5%) and the same holds for MRAC based PID controller with γ = 0.1 that has settling time > 2 s. Conversely, the MRAC based PID controller with γ = 0.2 to 20 meet the entire system performance specifications. In all cases, the system yielded zero steady state error.

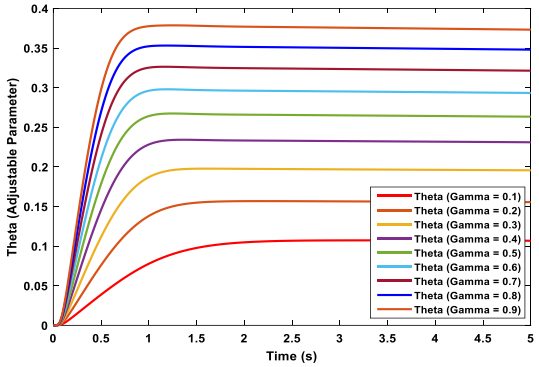

Fig. 9(a) Characteristic curves of adjustable parameter for varying gamma ($0.1 \leq \gamma \leq 0.9$)

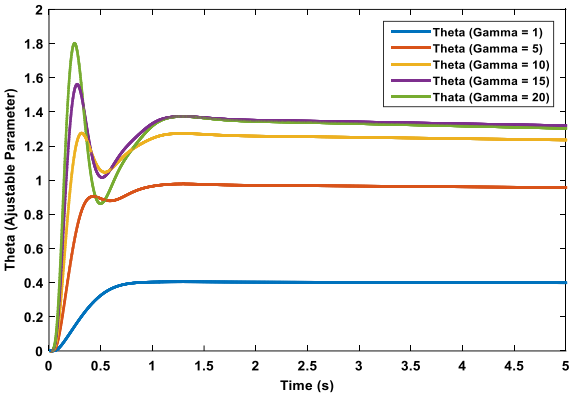

Fig. 9(b) Characteristic curves of adjustable parameter for varying gamma ($1 \leq \gamma \leq 20$)

TABLE 2.NUMERICAL VALUES OF ADJUSTABLE PARAMETER FOR DIFFERENT VALUES OF ADAPTION GAIN

Adaptation gain, Gamma (γ)	Adjustable parameter, Theta (θ_c)
0.1	0.1068
0.2	0.1555
0.3	0.1957
0.4	0.2311
0.5	0.2634
0.6	0.2933
0.7	0.3214
0.8	0.3480
0.9	0.3732
1	0.3990
5	0.9565
10	1.2350
15	1.3190
20	1.3030

The numerical values of the adjustable parameter that are produced by the various adaption gains of the MRAC based PID controller shown in Table 2 indicate that increasing adaption gain resulted in increasing value of adjustable parameter. The adjustable parameter is coordinated by the adjustment mechanism of the MRAC controller, which then alters the control command of the PID controller in order to ensure that the defined transient response characteristics of the reference model is constantly sustained and the model referenced followed. The relationship between γ and θ_c as shown in Table 2 agrees with (15) except for γ = 15 and 20

where it was altered, which can be attributed to turning point of $\mathbf{d\theta_c/dt}$ wherein the value of θ_c increases and then decreases. Hence, this turning point can be said to indicate optimal adaption gain region of the proposed MRAC algorithm.

In Fig. 10, the error voltage curves of the various system conditions reveal that for unit step input, the deviation between the desired yaw angle and the actual yaw angle reduces to zero as system reaches the expected satellite yaw-axis attitude.

Figure 11 clearly revealed that for each control system condition, the armature voltage drops to zero once the desired yaw angle is reached by the microsatellite. However, the numerical analysis indicated that the MRAC based PID controller with γ = 20 consumed the highest quantity of electrical energy expressed in terms of armature voltage (2281 V) during the control operation as shown in Table 3. Despite this shortcoming associated with the MRAC based PID control system with γ = 20, the proposed system offers improved energy consumption than the classical PID (New) controller for all other adaption gains.

In the case of generated motor torque as shown in Figure 12, it can be seen that the PID (New) controller yielded the highest value. Thus, from Table 3, the value was 53.13 Nm followed by 50.84 Nm for MRAC based PID controller with γ = 20. It suffices to say that the largest turning effect is experienced by the motor when PID controller is used. Generally, zero voltage is maintained by the armature including the motor torque once the desired yaw-angle is reached. This means that the motor stops when the actual yaw attitude equal to the desired yaw angle since the error signal reduces to zero resulting in no control action by the controller.

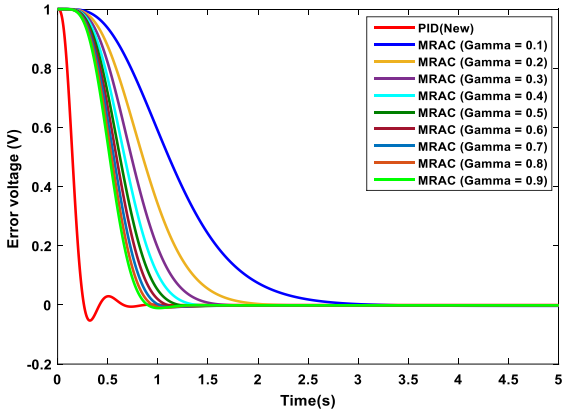

Fig. 10(a) .Error voltage curves for PID and MRAC ($0.1 \le \gamma \le 0.9$)

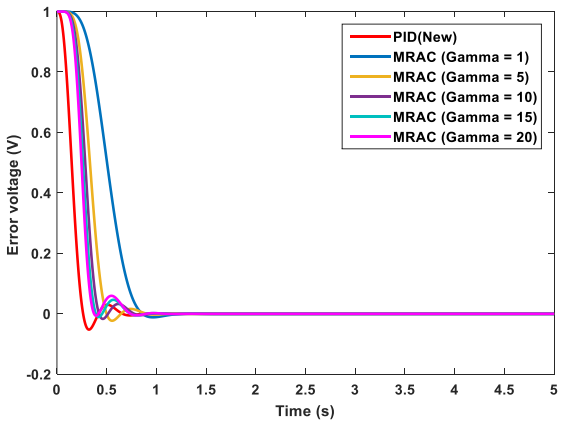

Fig. 10(b) Error voltage curves for PID and MRAC ($1 \le \gamma \le 20$)

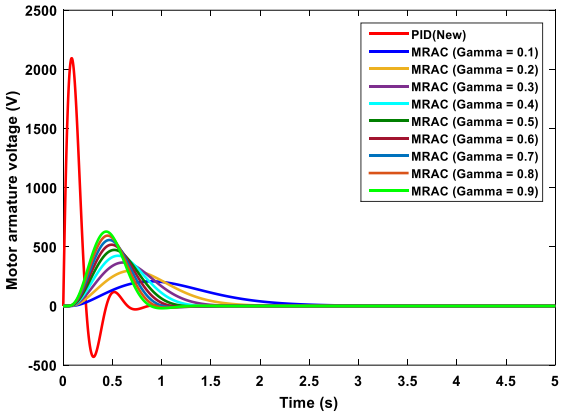

Fig. 11(a) Armature voltage curves for PID and MRAC ($0.1 \le \gamma \le 0.9$)

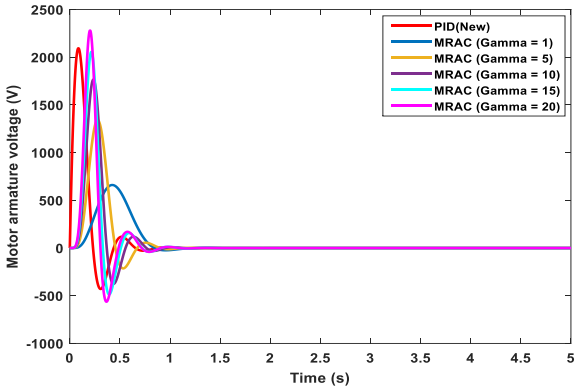

Fig. 11(b) Armature voltage curves for PID and MRAC ($1 \le \gamma \le 20$)

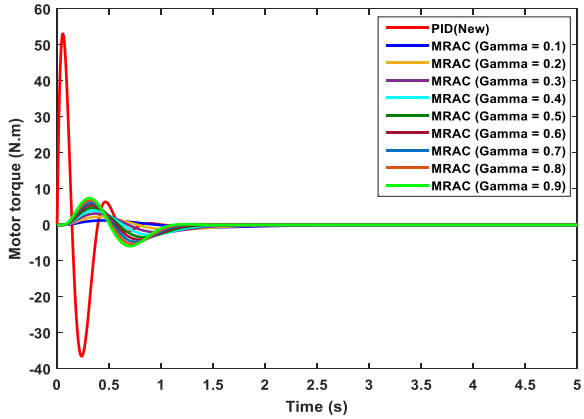

Fig. 12(a) Motor torque curves for PID and MRAC ($0.1 \le \gamma \le 0.9$)

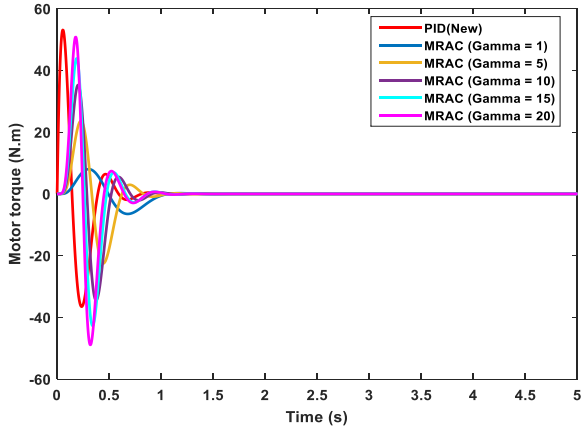

Fig. 12(b) Motor torque curves for PID and MRAC ($1 \le \gamma \le 20$)

TABLE 4. NUMERICAL VALUES OF OPTIMAL PARAMETERS

MRAC based PID Controller	ISE	IAE	ITAE
MRAC (Gamma = 0.1)	0.8936	1.185	0.8497
MRAC (Gamma = 0.2)	0.6928	0.8934	0.4768
MRAC (Gamma = 0.3)	0.6043	0.7666	0.3494
MRAC (Gamma = 041)	0.5510	0.6915	0.2840
MRAC (Gamma = 0.5)	0.5142	0.6406	0.2438
MRAC (Gamma = 0.6)	0.4868	0.6031	0.2163
MRAC (Gamma = 0.7)	0.4653	0.5739	0.1962
MRAC (Gamma = 0.8)	0.4478	0.5504	0.1807
MRAC (Gamma = 0.9)	0.4332	0.5308	0.1683
MRAC (Gamma = 1)	0.4217	0.5156	0.1591
MRAC (Gamma = 5)	0.2829	0.3383	0.07187
MRAC (Gamma = 10)	0.2442	0.2923	0.05569
MRAC (Gamma = 15)	0.2254	0.2717	0.04959
MRAC (Gamma = 20)	0.2136	0.2603	0.04694

The optimal adaption gain determined in terms of minimum error analysis performed considering ISE, IAE and ITAE as shown in Table 5 revealed that the MRAC based PID controller with $\gamma = 20$ offered the best performance in terms of reduced error during control process such that ISE = 0.2136, IAE = 0.2603 and ITAE = 0.04694 among all the adaption gains. This is followed by the MRAC based PID controller with $\gamma = 15$ and subsequently, with $\gamma = 10$. Hence, the MRAC based PID control system with $\gamma = 10$, 15, and 20 are used to carry out performance comparison with previous control schemes applied to the same microsatellite yaw-axis ACS studied in [5].

C. Comparison with Previous Techniques

Simulation curves and the numerical analysis from the performance comparison of the proposed system against the previous control techniques for the microsatellite yaw-axis ACS in [5] are presented in this section as shown in Figure 13 and Table 5. These previous control schemes are PID controller tagged PID (Exist), PID with pre-filter, PD, and PD with pre-filter.

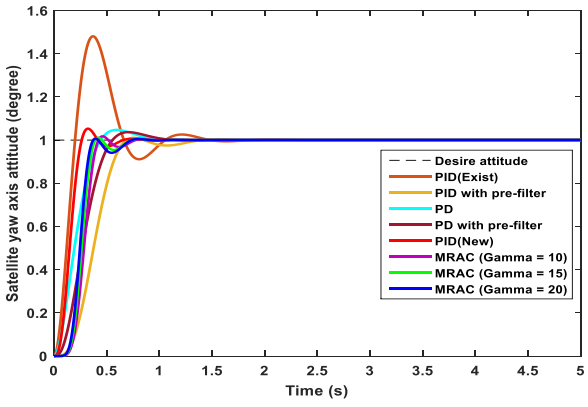

Fig. 13. Step response comparison

TABLE 5. COMPARISON OF STEP RESPONSE CHARACTERISTICS

System condition	t_r *(s)*	t_s *(s)*	M_p *(%)*	t_p *(s)*	e_{ss} *(degree)*
PID (Exist)	0.14	1.31	48.05	0.37	0
PID with pre-filter	0.37	1.17	1.08	0.76	0
PD	0.29	0.81	4.73	0.59	0
PD with pre-filter	0.33	0.89	3.66	0.71	0
PID (New)	0.16	0.57	5.25	0.32	0
MRAC (gamma = 10)	0.18	0.69	1.67	0.46	0
MRAC (gamma = 15)	0.16	0.67	1.07	0.42	0
MRAC (gamma = 20)	0.15	0.67	0.64	0.39	0

Considering the simulation curves of the various system conditions shown in Figure 13 and the numerical analysis in Table 5, it can be seen that the PID (Exist) and PID (New) controllers did not meet all the expected system performance criteria specifically the maximum overshoots, which were greater than 5%. But for other system conditions, the controllers achieved the expected performance criteria. Furthermore, looking at the table, it is obvious that the proposed MRAC based PID controller with $\gamma = 10$, 15, and 20 outperformed the other control systems in terms of overall transient response characteristics regarding the defined system performance criteria.

IV. CONCLUSION

In this paper, an MRAC based PID controller for microsatellite yaw-axis attitude control system using approximated second order technique has been presented. The proposed control system was modelled and simulated in MATLAB/Simulink environment. The proposed MRAC algorithm provided a wide range of adaptation gain that can be utilized by the system to provide adaptive scheme for ACS. Simulation results indicated that MRAC based PID controller met the system performance criteria for adaption gain, $\gamma = 0.2$ to 20. An optimal performance in terms of error indices based on ISE, IAE and ITAE revealed that at $\gamma = 15$ and 20 the system provided finest response. In terms of energy consumption defined in terms of armature voltage, the proposed system outperformed classical PID controller except for $\gamma = 20$. When compared to previous PID and PD based control systems in Table 5, the MRAC based PID controller outperformed other controllers for all the performance criteria with $\gamma = 10$, 15, and 20. However, the choice of either MRAC based PID controller with $\gamma = 15$ or 20 should be made between the advantage of performance criteria defined in terms of settling time, maximum overshoot and steady-state error over the cost of energy consumption or otherwise. Generally, if the cost of energy consumption is to be considered together with meeting the defined transient response characteristics, the MRAC based PID controller with $\gamma = 0.2$ to 15 should be implemented over PID controller.

ACKNOWLEDGMENT

Authors are thankful to the management of the Department of Electrical and Electronic Engineering, Imo State University, for availability afforded them in utilizing the electronic and control laboratory during this study.

REFERENCES

[1] Y. Shan, L. Xia and S. Li, "Design and simulation of satellite attitude control algorithm based on PID," *Journal of Physics: Conference Series*, vol. 2355, no. 012035, pp. 1-9, 2022. DOI: 10.1088/17426596/2355/1/012035.

[2] Y. Qi, H. Jing and X. Wu, "Variable structure PID controller for satellite attitude control considering actuator failure," *Applied Science*, vol. 12, no. 5273, pp. 1-19, 2022. DOI:10.3390/app12105273

[3] H. Travis, "Introduction to satellite attitude control," in *Advances in Spacecraft Attitude Control*, IntechOpen, 2020. DO:10.5772/intechopen.89658

[4] C. C. Mbaocha, C. U. Eze, I. A. Ezenugu and J. C. Onwumere, "Satellite model for yaw-axis determination control using PID

compensator," *International Journal of Scientific & Engineering Research,* vol. 7, no. 7, pp. 1623-1629, 2016.

[5] A. T. Ajiboye, J. O. Popoola, O. Oniyide and S. L. Ayinia, "PID controller for microsatellite yaw-axis attitude control system using ITAE method," *TELKOMNIKA Telecommunication, Computing, Electronics and Control*, vol. 18, no. 2, pp. 1001-1011, 2020. DOI:10.12928/TELKOMNIKA.v18i2.14303

[6] E. U. Enejor, F. M. Dahunsi, K. F. Akingbade and I. O. Nelson, "Low earth orbit satellite attitude stabilization using linear quadratic regulator," *European Journal of Electrical and Computer Science*, vol. 7, no. 3, pp. 17-29, 2023. DOI:10.24018/ejece.2023.7.3.505

[7] A. Bello, K.S. Olfe, J. Rodríguez, J. M. Ezquerro and V. Lapuerta, "Experimental verification and comparison of fuzzy and PID controllers for attitude control of nanosatellites," *Advances in Space Research,* vol. 71, pp. 3613-3630, 2023. DOI:10.1016/j.asr.2022.05.055

[8] K. M. Portella, W. N. Schinestzki, R. M. Sehnem, L. B. Luz, L. Q. Mantovani, R. R. Sacco, T. K. S. Sartori and P. Paglione , " Satellite attitude control using control moment gyroscopes," *Journal of Aerospace Technology and Management, São José dos Campos,* vol. 12, pp. 94-105, 2020. DOI:10.5028/jatm.cab.1156

[9] J. Narkiewicz, M. Sochacki and B. Zakrzewski, "Generic model of a satellite attitude control system," *International Journal Aerospace Engineering*, vol. 2020, pp. 1-17, 2020. DOI:10.1155/2020/5352019

[10] A. D. Dass, H. Sanusi and A. M. Muad, "Stabilizing roll, pitch and yaw angles for attitude control system (ACS) using direct torque control (DTC)," *International Journal of Advanced Trends in Computer, Science and Engineering*, vol. 8, no. 1.6, pp. 263-267, 2019. DOI:10.30534/ijatcse/2019/3981.62019

[11] M. Okasha, M. Idres and A. Ghaffar, "Satellite attitude tracking control using Lyapunov control theory," *International Journal of Recent Technology and Engineering*, vol. 7, no. 6S, pp. 253-257, 2019.

[12] L. Jin and Y. Li, "Model predictive control-based attitude control of under-actuate spacecraft using solar radiation pressure," *Aerospace*, vol. 9, no. 498, pp. 1 – 20, 2022. DOI:10.3390/aerospace9090498

[13] B. C. Agwah and P. C. Eze, "An intelligent controller augmented with variable zero lag compensation for antilock braking system," *International Journal of Mechanical and Mechatronic Engineering*, vol. 16, no. 11, pp. 303-310, 2022.

[14] P. C. Eze, B. O. Ekengwu, N. C. Asiegbu and T. I. Ozue, "Adjustable gain enhanced fuzzy logic controller for optimal wheel slip ratio tracking in hard braking control system," *Advances in Electrical and Electronic Engineering*, vol. 19, no. 3, pp. 231-242, 2021. DOI: 10.15598/aeee.v19i3.4124

[15] A. Fattah, "Design and analysis of speed control using hybrid PID-Fuzzy controller for induction motors," M.S. thesis, Dept. Elect. Comput. Eng., Western Michigan Univ., Kalamazoo, Michigan, 2015.

[16] H. Liu, Q. Yu and Q. Wu, "PID control model based on back propagation neural network optimized by adversarial learning-based grey wolf optimization," *Applied Science*, vol. 13, no. 4767, pp. 1-21, 2023. DOI:10.3390/app13084767

[17] M. A. Si Mohammed, "Simulation of three axis attitude control using a control momentum gyroscope for small satellites," *Proceeding of the World Congress Engineering*, London, U. K., pp. 896-901, 2012.

[18] P. C. Eze, C. A. Ugoh, C. P. Ezeabasili, B. O. Ekengwu and L. E. Aghoghovbia, "Servor position control in hard disk drive of a computer using MRAC integrating PID algorithm," *American Journal of Science, Engineering and Technology*, vol. 2, no. 4, pp. 97-105, 2017. DOI:10.11648/j.ajset.20170204.11

[19] A. Daiifarshchi and S. Bargandan, "Design of a model reference adaptive controller using modified MIT rule for a second order system," *Journal of Artificial Intelligence in Electrical Engineering*, vol. 7, no. 25, pp. 7-14, 2018